Dual Spectrometer for Simultaneous Visible and Extreme Ultraviolet LIBS

Di Qu*[ab], Matthias Trottmann[a], Corino Wyder[a], Davide.Bleiner[a]
[a]Swiss Federal Laboratories for Materials Science and Technology, Ueberlandstr. 129, 8600 Dübendorf; [b]DUniversity of Zurich, Department of Chemistry, Winterthurstr. 190, CH8057 Zurich, Switzerland

ABSTRACT

Laser-induced breakdown spectroscopy (LIBS) is an elemental analysis method thanks to minor sample preparation, rapid analysis, and a spatially resolved sensitivity down to trace level in any kind of sample matrix. State-of-the-art LIBS is operated in the optical spectral range (UV-Vis). Unfortunately, the application of LIBS in material detection is limited by the low precision and repeatability. This is particularly critical for inhomogeneous materials and alternative methods are desirable. Light elements such as Li, as well as F, are difficult to be characterized. The dual LIBS performance was initially studied in a simpler matrix such as LiF, radially collecting simultaneously the XUV and OES spectra from the same laser shot. For the case of LiF, XUV signals proved significantly more stable than in the case of LIBS-OES. The signal of F can be also seen clearly in the spectrum. Observation of the plasma emission at even shorter wavelengths in the extreme ultraviolet (wavelength range 5-20 nm) is supposed to improve the state-of-art limitations of LIBS.

Keywords: Laser induced plasma, Laser induced breakdown spectroscopy, XUV emission spectroscopy

1. INTRODUCTION

Laser Induced Breakdown Spectroscopy (LIBS) is a widely studied technique for elemental analysis that requires little to no sample preparation [1–4]. The intense laser pulse was focused on the target surface to induce a micro-plasma, which consists of excited atoms, ions, molecules or particles. The optical emission from the laser-induced plasma can be collected with a spectrometer for the further elemental or chemical analysis. Thus, LIBS also offers the compelling advantages of fast detection speed, high spatial resolved sensitivity up to trace levels in any type of sample matrix[2,3,5–7], as well as broad element coverage from light to heavy element detection. So far, much work has focused on the LIBS for elemental and quantitative analysis in the wavelength range from VUV [8] to UV-VIS [5,7,9,10]. Nevertheless, LIBS has also a few unavoidable limitations, such as high uncertainty of the signal, poor precision and repeatability of the signal because of the shot-to-shot fluctuations and noise [1,11,12]. The noise can be classified into four sources of noise: (i) source noise due to the inhomogeneity in the sample or else the laser-plasma interaction and plasma evolution; (ii) shot noise generated by the number of photons arriving on the detector; (iii) the detector noise; (iv) the instrumental (thermal) drift [11]. It was shown previously, that one may mitigate the signal fluctuation by increasing the number of laser pulses accumulated in the spectra[11]. It was also reported that double-pulse irradiation has improved the signal-to-noise ratio in LIBS [13]. Moreover, an interesting hyphenated approach to enhance the signal and LIBS's sensitivity and stability, was also introduced, where the LIBS was coupled with Raman spectroscopy [14].

Recently, the light element lithium has attracted much attention thanks to its application in energy material [15]. However, the detection and chemical analysis of Li are still limited. For instance, there is still a challenge for detecting oft X-rays at 55 eV as the K Li-edge in energy dispersive X-ray spectroscopy (EDX) [16]. In fact, it has been reported that the hydrogen-like Li^{2+} (Li III) has a strong emission line at λ =13.5 nm showing a potential application in laser-produced plasma XUV source [17,18]. Hence, the emission line from Li III at 13.5 nm might provide a new pathway for Li detection and chemical analysis of Li containing materials in LIBS. LIBS of Li containing materials in the XUV wavelength range (5-20 nm) has not been presented based on our knowledge. In the present study, Li fluoride (LiF) is taken as a test material that contains only two elements. LiF is an important optical material[19,20], as well as a salt in electrolyte or as protective layer on the electrolyte/electrode interface [21].

The aim of this work was to investigate an alternative detection range, to improve the precision of LIBS, i.e. collecting radiation at a much shorter wavelength than what conventionally carried out. The LIBS-XUV setup was performed with the LiF sample. The paper is organized as follows: section 2 introduces the experimental setup. Section 3 discusses the

International Conference on X-Ray Lasers 2020, edited by Davide Bleiner,
Proc. of SPIE Vol. 11886, 118860X · © 2021 SPIE · CCC code:
0277-786X/21/$21 · doi: 10.1117/12.2594458

experimental results comparing the precision of LIBS-XUV and LIBS-OES, as well as the slit width effect on the XUV signal. Section 4 contains the conclusion with an outlook on possible further studies.

*Di.Qu@empa.ch;

2. EXPERIMENTAL

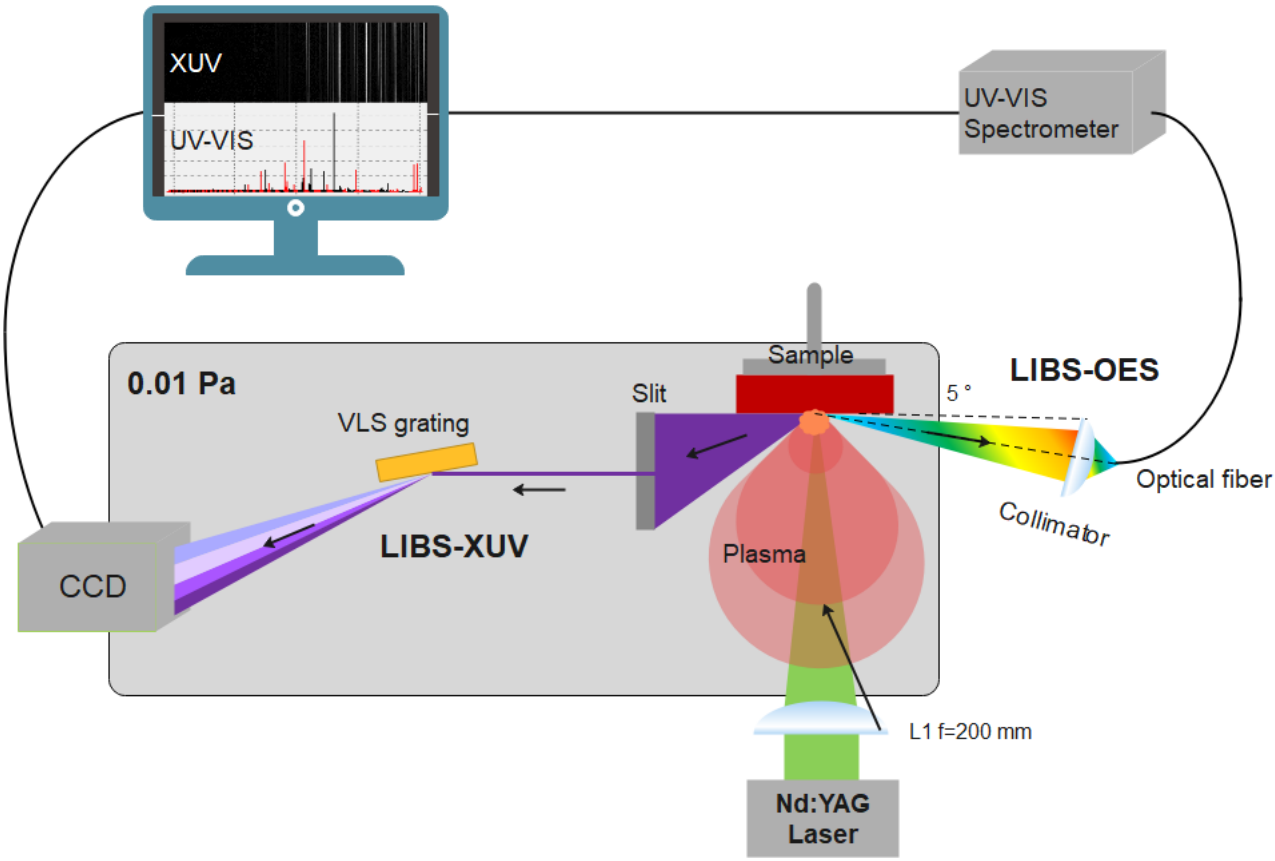

Figure 1 The LIBS-XUV and LIBS-OES setup. The laser beam (λ =532 nm) is focused with a lens (L1) placed in the air. The target material and XUV spectrometer are placed in the vacuum chamber. The LIBS-OES signal and LIBS-XUV signal are collected radially with a fiber optic and flat-field XUV spectrometer, respectively.

2.1 Instrument

The laser beam is generated from a second harmonics Q-switched Nd:YAG laser source(λ=532nm, Q-smart, Lumibird) with a pulse duration of 5 ns, repetition rate 10 Hz and a pulse energy of 100 mJ for plasma ignition. As shown in **Fig. 1**. The laser beam was focused with lens L1 (LA1253, Thorlabs, f=200 mm) about 1 mm below the sample surface and the laser spot size is approximately 200 µm. The sample surface is perpendicular to the laser beam to generate a homogeneous ablation. The pulse-to-pulse fluctuation in laser energy is <5%.

The emission from the plasma plume can be radially collected by using a collimator (Avantes, COL-UV/VIS) and an optical fiber (Ocean Optics), then guided into an echelle UV-VIS spectrometer (Aryelle 200 LTB Berlin, Germany). The ICCD camera (ANDOR iStar) is attached to the OES spectrometer to collect the LIBS spectra. The wavelength range of the measured spectrum is 190.01– 603.89 nm. The LIBS-OES signals were acquired with a delay time of 0.2 µs to the laser pulse, and a gate width (camera integration time) of 10 µs.

On the other hand, the LIBS-XUV is acquired from an XUV spectrometer in the radial direction of the laser-induced plasma. The XUV spectrometer consists of a collimation slit, a gold-coated concave variable-line-spacing (VLS) grating

(Hitachi model 001-0437) and a back-illuminated X-ray CCD detector (Greateyes GE2048 512 BI UV1). The schematic of the spectrometer is shown on the left side in **Fig 1**. In order to get a sharp spectrum on the CCD camera, the slit was adjusted to 50 µm. The incident angle needs to be carefully adjusted to a specific standard setting value (87°) as explained in a previous publication [22]. The back-illuminated CCD is placed vertically at the focal plane of the spectrometer after the grating to collect the XUV spectrum. The CCD sensor has a 2048 x 512 array with a pixel size of 13.5 x 13.5 μm^2. The wavelength calibration of the XUV spectrum can also be found in the ref. [22].The laser ablation and XUV spectrometer must be operated within the low pressure system because of the absorption of XUV in air, at an operating pressure of 10 mPa.

2.2 Sample material

Regarding to the Li detection in battery material with for later LIBS study, LiF was first chosen as a reference material due to the detection challenge put forward by the elements Li and fluorine (F). It is known that there are only three electrons in the Li atomic shells. As a result, the number of transitions of neutral and ionic Li is much lower than that of heavier elements. In particular, it is known that Li III has a strong emission line at λ =13.5 nm [18]. The 2-inch LiF plate had a thickness of 4 mm, which was supplied by Golem IMS GmbH.

3. RESULT AND DISCUSSION

3.1 LIB-XUV and LIBS-OES spectra

The emission spectra of LiF in the XUV and OES ranges from laser-induced plasma were recorded simultaneously. In order to provide reliable result, the average of 20 emission spectra in both spectral domains are presented for a LiF plasma, as shown in **Fig. 2.a** and **Fig. 2.b**. There is an interesting finding that the strongest emission lines in both spectral ranges were generated from the Li species, such as Li III line at λ =13.5 nm at in XUV and Li I line at λ =460.3 nm in OES. These two strongest lines showed a promising opportunity for LIBS analysis of Li in Li-containing materials. The Li III line at 13.5 nm corresponds to the 1s-2p transition and the Li I line at 460.3 nm corresponds to the $1s^22p$-$1s^24d$ transition. Moreover, the Li III line at λ =11.4 nm and the Li II line at λ =16.7 nm were also observed in the LIBS-XUV. Beside to the Li lines, there are also several obvious emission lines from the F VI and F VII distributed in the wavelength range of 9-15 nm. In the LIBS-OES spectrum, the strong transitions are generated from the neutral and singly ionized Li and F atom. It is evident that the transitions from higher ionization stages are observed by LIBS-XUV that cannot be obtained in the LIBS-OES. Moreover, LiF have great potential as a fuel material in application of EUV lithography. Because the laser-induced LiF plasma shows a pure emission line from Li III at 13.5 nm that was the working wavelength for state-of-art EUV lithography[17,18].

During the measurement, it was observed that the line intensity from LIBS-OES are not stable as that from LIBS-XUV. In order to demonstrate this phenomenon, the line of Li III at λ=13.5 nm was selected for investigations of the stability of LIBS-XUV, as well as the line of Li I at λ= 460.3 nm for LIBS-OES. The selection of the reference line with highest intensity is necessary to avoid the effect of shot-noise from the detector. 20 laser pulses were subsequently delivered to the LiF sample with the same laser energy (100 mJ) to obtain more insight on the precision of the LIBS-OES and LIBS-XUV measurements. The evolution of the Li III line intensities by 20 single laser shot is plotted in **Fig. 2.c.** Simultaneously, the evolution of the Li I line intensities by the same 20 single laser shot is shown in **Fig. 2.d.** The line intensities of both lines are not stable and fluctuated randomly. Generally, the precision of the measurements can be statistically evaluated by the relative standard deviation (RSD) of the line intensity. Hence, the repeatability of the LIBS is given by the formula:

$$RSD = \frac{\sigma_I}{\bar{I}} = \frac{\sqrt{\frac{1}{n}\sum_{i=1}^{n}(I_i - \bar{I})^2}}{\bar{I}} \quad (1)$$

Where *I* is the line intensity from the spectra and *n* is the number of repetitions of the experiments. As shown in **Fig. 2.c and Fig 2.d**, the relative standard deviation (RSD) of Li III in XUV and Li I in OES are 7.1% and 23.1%, respectively. The resulting 23.1% RSD of line intensity coincide with the result from [12]. Fu et al. has reported that the significant LIBS spectral signal fluctuation is attributed to the plasma morphology or plasma evolution, total number of density, as well as the delay time. The plasma morphology shows a poor repeatability at later stage of the plasma, which required an appropriate delay time of the acquiring of LIBS signal. Meanwhile, the signal of LIBS-OES mainly comes from the aged stage of laser-induced plasma, which results in the poor stability and precision of LIBS-OES. On the contrary, the XUV is generated during the very early stage of the laser-induced plasma, which shows a much higher stability and precision.

In fact, the low precision and uncertainty of LIBS-OES have been reported and studied in previous works [17][18]. The larger fluctuation in LIBS-OES might be mainly caused by the shot noise and the source noise. The shot noise is defined as the random number of photons arriving on the detector during the acquiring time. An ICCD detector was applied in LIBS-OES and a CCD detector was applied in LIBS-XUV, where the light collection efficiencies are very different during the measurement, according to the different slit width as well as the gain of a MCP (Micro-Channel Plate) in an ICCD. In order to reduce the contribution of the shot noise to the total RSD of the measurements, the highest possible signal intensity must be reached by optimizing the experimental conditions [11]. On the other hand, the source noise can affect all the spectral features to some extent, such as the occurrence of transitions and continuum emission [11]. The source noise, namely flicker noise, is generated from the laser sample or laser plasma interaction[11]. Plasma inhomogeneity and zoning may also contribute to erratic signals in the LIBS data. The phenomenon of signal disappearance occurred in LIBS-OES referring to a poor repeatability and uncertainty. However, LIBS-XUV showed very good repeatability that signal was always occurred in all experiments. On the basis of these result, one can conclude that LIBS-XUV showed a better precision than LIBS-OES, with a RSD as low as 7.1%, as well as a better repeatability.

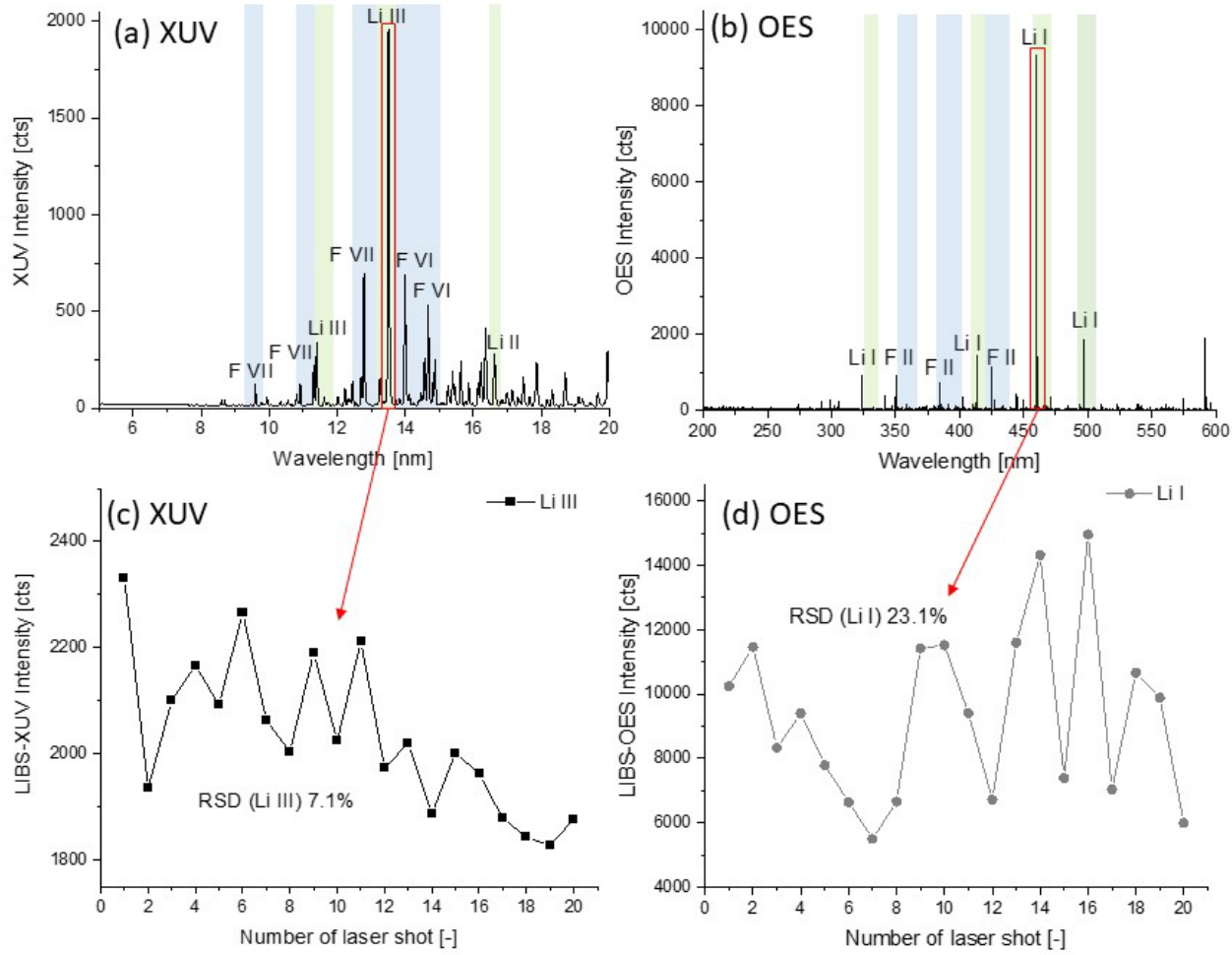

Figure 2 Average spectrum of 20 LIBS spectra (a) in XUV range and (b) OES from laser-induced LiF plasma. (c) Plot of the line intensities of Li III at 13.5 nm in the LIBS-XUV spectra, which were obtained from the 20 laser shots in single-shot mode. (d) Plot of the line intensities of Li I at 460.3 nm in the LIBS-OES spectra, which were generated from the 20 laser shots in single-shot mode. Relative standard deviations (RSD) of the line intensities are given in the plot.

3.2 Effect of slit width on the XUV spectrum

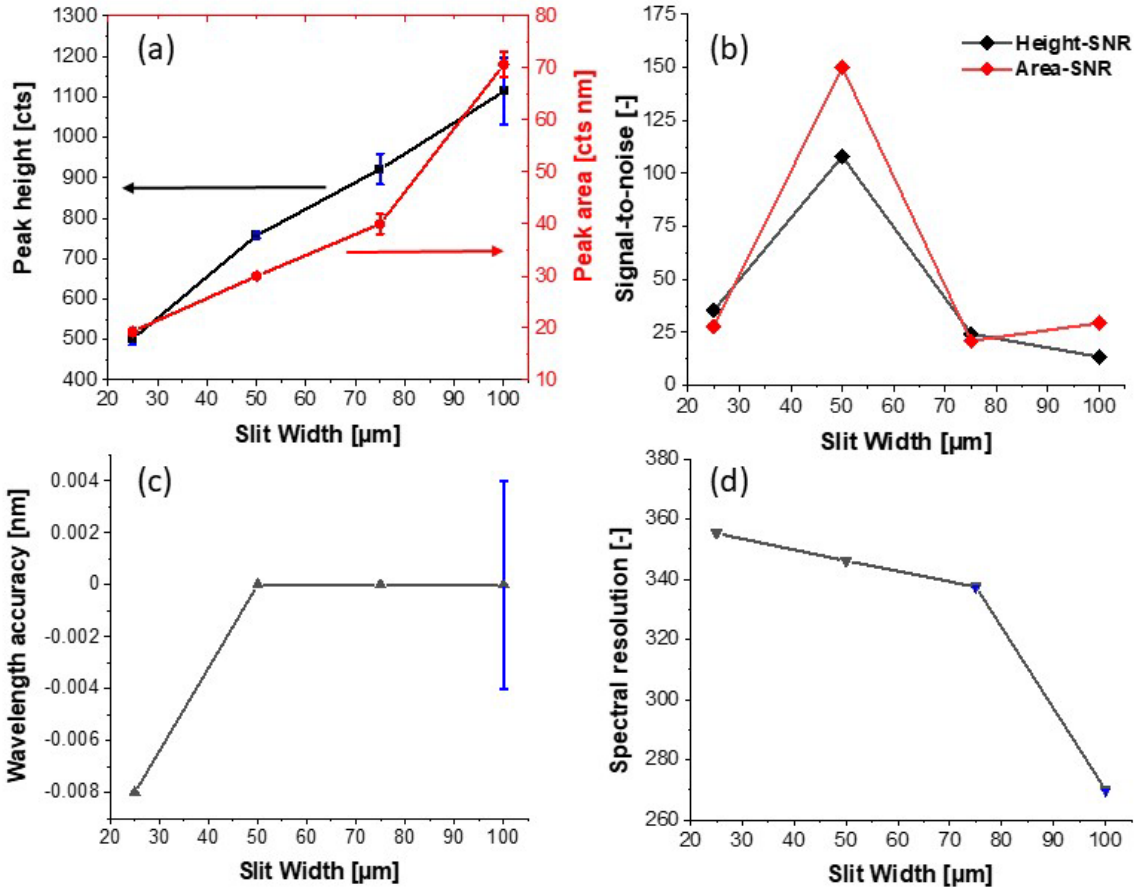

Figure 3 Slit width effect on the line (a) Peak height (intensity) and peak area. (b) Signal-to-noise ratio of peak height and peak area. (c) Wavelength accuracy stands for the deviation of central wavelength to the theoretical wavelength. (d) Resolving power (λ/Δλ) of the line Li III at 13.5 nm. The error bars give the standard deviation of each slit width

The spectral lines are collected as dispersive images of the laser-plasma with the XUV spectrometer. The collimation slit width of the XUV spectrometer plays an important role for the resolution and intensity of a collected spectrum. The observed effect of slit width on the XUV spectrum is summarized in **Fig. 3**. The measurements were carried out on the LiF sample with slit widths of 25 µm, 50 µm, 75 µm and 100 µm. The laser energy was 100 mJ and every spectrum was obtained by averaging n=3 experimental results for each slit width. The emission line Li III at λ =13.5 nm was selected to deliver the slit width effect on the spectral line. **Fig. 3.a** shows the correlation between the peak height (line intensity) and the slit width, as well as the peak area and the slit width. Obviously, as the slit width increases, the intensity and peak area also increase.

The peak height-to-noise and the peak area-to-noise ratio are shown in **Fig. 3.b**. The standard deviation of three measurement for each slit width is regarded as the noise. The slit width of 50 µm gives highest signal to noise ratio (SNR). Furthermore, the peak area SNR showed an increase of nearly 40% compared to the peak height SNR, showing that the peak area yields a more robust result.

In addition, the wavelength accuracy and spectral resolution have been also plotted in **Fig. 3.c** and **Fig. 3.d**. The wavelength accuracy represents the absolute deviation of the measured center wavelength of the peak from the theoretical wavelength of λ = 13.5 nm, where the central wavelength from 25 µm slit width deviates from the theoretical value. The resolving powers (λ/Δλ) of the Li III peak with slit width of 25 µm, 50 µm, 75 µm and 100 µm are 355.3, 346.2, 337.5 and 270.0, respectively. These are corresponding to the FWHM (Δλ, Full Width Half Maximum) of 0.038, 0.039, 0.040 and 0.050, respectively.

Even though a narrow slit width of 25 µm shows the highest relative spectral resolution, the intensity of the spectral lines is also greatly reduced to only 500 counts. This will cause an elimination below the SNR of several weak spectral lines and incompleteness of the spectral information. Moreover, the central wavelength of Li III with a slit width of 25 µm is deviated from the theoretical value 13.5 nm, possibly due to mechanical alignment issues. It must be mentioned by construction, only one knife-edge of the slit edges in XUV spectrometer can be translated, which can result in the shift of center line-of-sight. This is the central wavelength of observation. In addition, it is obvious that the measurement standard deviation increases as the slit width increases. Therefore, regarding to the abovementioned factors, the slit width of 50 µm was selected as the optimum slit width for the further experiments.

4. CONCLUSIONS

A dual spectrometer for simultaneous LIBS-XUV and LIBS-OES was presented with LiF in this present work. LIBS-XUV is an innovative method for element analysis in solid samples, which collected the XUV spectral emission of a laser-produced plasma. Li III has a stable and intensive emission line at 13.5 nm which can be used as the reference line for LIBS-XUV analysis. Simultaneously, the Li I shows a emission line at 460.3 nm showing also the ability for the lithium detection. However, the line intensity of Li III in the LIBS-XUV is much more stable and precise than that of Li I in the conventional LIBS-OES. In addition, the effect of slit width in the XUV spectrometer was also investigated, where a 50 µm slit width gave the best compromise between precision and sensitivity. Observation of the plasma emission at even shorter wavelengths in the extreme ultraviolet (wavelength range 5-20 nm) is supposed to improve the state-of-art precision of LIBS. As a future work, we are considering the use of tabletop X-ray lasers (see also Sects. 1-4 [23]) as a LIBS pump.

REFERENCES

1. Hahn, D. W. & Omenetto, N. Laser-Induced Breakdown Spectroscopy (LIBS), Part II : Review of Instrumental and Methodological Approaches to Material Analysis and Applications to Different Fields. *Appl. Spectrosc.* **66**, 347–419 (2012).
2. Smyrek, P., Electrochem, J., Soc, A., Smyrek, P. & Pr, J. Laser-Induced Breakdown Spectroscopy of Laser-Structured Li (NiMnCo) O 2 Electrodes for Lithium-Ion Batteries Laser-Induced Breakdown Spectroscopy of Laser-Structured Li (NiMnCo) O 2 Electrodes for Lithium-Ion Batteries. *J. Electrochem. Soc.* **163**, A19–A26 (2016).
3. Smyrek, P., Bergfeldt, T., Seifert, H. J. & Pfleging, W. Laser-induced breakdown spectroscopy for the pro fi les in structured and unstructured electrodes. *J. Mater. Chem. A* **7**, 5656–5665 (2019).
4. Windom, B. C., Diwakar, P. K. & Hahn, D. W. Dual-pulse Laser Induced Breakdown Spectroscopy for analysis of gaseous and aerosol systems: Plasma-analyte interactions. *Spectrochim. Acta - Part B At. Spectrosc.* **61**, 788–796 (2006).
5. Imashuku, S. *et al.* Quantitative lithium mapping of lithium-ion battery cathode using laser-induced breakdown spectroscopy. *J. Power Sources* **399**, 186–191 (2018).
6. Hou, H. *et al.* Three-dimensional elemental imaging of Li-ion solid-state electrolytes using fs-laser induced breakdown spectroscopy (LIBS). *J. Anal. At. Spectrom.* **30**, 2295–2302 (2015).
7. He, Y. *et al.* Lithium ion detection in liquid with low detection limit by laser-induced breakdown spectroscopy. *Appl. Opt.* **58**, 422–427 (2019).
8. A. Khater, M., Costello, J. T. & Kennedy, E. T. Optimization of the Emission Characteristics of Laser-Produced Steel Plasmas in the Vacuum Ultraviolet : Signi cant Improvements in Carbon Detection Limits. *Appl. Spectrosc.* **56**, 970–983 (2002).
9. Indrizzi, L., Ohannessian, N., Pergolesi, D., Lippert, T. & Gilardi, E. Pulsed Laser Deposition as a tool for the development of all solid-state microbatteries. *Helv. Chim. Acta* (2020). doi:10.1002/hlca.202000203
10. Imashuku, S. *et al.* Quantitative lithium mapping of lithium-ion battery cathode using laser-induced breakdown spectroscopy. *J. Power Sources* **399**, 186–191 (2018).
11. Tognoni, E. & Cristoforetti, G. Signal and noise in Laser Induced Breakdown Spectroscopy : An introductory review Optics & Laser Technology Signal and noise in Laser Induced Breakdown Spectroscopy : An introductory review. *Opt. Laser Technol.* **79**, 164–172 (2015).

12. Fu, Y., Hou, Z., Li, T., Li, Z. & Wang, Z. Investigation of intrinsic origins of the signal uncertainty for laser-induced breakdown spectroscopy. *Spectrochim. Acta - Part B At. Spectrosc.* **155**, 67–78 (2019).
13. Babushok, V. I., DeLucia, F. C., Gottfried, J. L., Munson, C. A. & Miziolek, A. W. Double pulse laser ablation and plasma: Laser induced breakdown spectroscopy signal enhancement. *Spectrochim. Acta - Part B At. Spectrosc.* **61**, 999–1014 (2006).
14. Hoehse, M., Gornushkin, I., Merk, S. & Panne, U. Assessment of suitability of diode pumped solid state lasers for laser induced breakdown and Raman spectroscopy. *J. Anal. At. Spectrom.* **26**, 414–424 (2011).
15. Li, M., Lu, J., Chen, Z. & Amine, K. 30 Years of Lithium-Ion Batteries. *Adv. Mater.* **30**, 1–24 (2018).
16. Hovington, P. *et al.* Can we detect Li K X-ray in lithium compounds using energy dispersive spectroscopy? *Scanning* **38**, 571–578 (2016).
17. Tallents, G., Wagenaars, E. & Pert, G. Optical lithography: Lithography at EUV wavelengths. *Nat. Photonics* **4**, 809–811 (2010).
18. Bartnik, A. *et al.* Laser-produced plasma EUV source based on tin-rich , thin-layer targets. *Appl. Phys. B Lasers Opt.* **102**, 559–567 (2011).
19. Baig, M. A., Qamar, A., Fareed, M. A., Anwar-ul-Haq, M. & Ali, R. Spatial diagnostics of the laser induced lithium fluoride plasma. *Phys. plasma* **19**, 063304 (2012).
20. Todd Kvamme, E., Earthman, J. C., Leviton, D. B. & Frey, B. J. Lithium fluoride material properties as applied on the NIRCam instrument. in *Proc. SPIE 5904, Cryogenic Optical Systems and Instruments XI* **5904**, 59040N (2005).
21. Fan, X. *et al.* Fluorinated solid electrolyte interphase enables highly reversible solid-state Li metal battery. *Sci. Adv.* **4**, 1–11 (2018).
22. Qu, D. & Bleiner, D. Extreme ultraviolet plasma spectroscopy of a pseudospark XUV source. *J. Anal. At. Spectrom.* **35**, 2011–2022 (2020).
23. D. Bleiner, The Science and Technology of X-ray Lasers: A 2020 Update Proc. SPIE 11886, 1188602 (2021)